

# Progress on quantum transport simulation using empirical pseudopotentials

Jingtian Fang\*, William Vandenberghe, and Massimo Fischetti

The University of Texas at Dallas, 800 W. Campbell Road, Richardson, Texas 75080 USA

\*Email: jingtian.fang@utdallas.edu

## I. INTRODUCTION

After performing one-dimensional simulation of electron transport in narrow quantum wires without gate control in Ref [1], [2] using the open boundary-conditions full-band plane-wave transport formalism derived in Ref [3], we now extend the work to simulate three-dimensionally field-effect transistors (FETs) with a gate bias applied and obtain their transport characteristics. We optimize multiple procedures for solving the quantum transport equation (QTE), such as using a selected eigenvalue solver, the fast Fourier transform (FFT), block assignment of matrices, a sparse matrix solver, and parallel computing techniques. With an expanded computing capability, we are able to simulate the transistors in the sub-1 nm technology node as suggested by the ITRS [4], which features  $\sim 5$  nm physical gate length,  $\sim 2$  nm body thickness,  $\sim 0.4$  nm effective oxide thickness (EOT),  $\sim 0.6$  V power supply voltage, and a multi-gate structure. Here we simulate an armchair graphene nanoribbon (aGNR) FET using a gate-all-around architecture and obtain its transport properties. We will discuss the numerics concerning the matrix size of the transport equation, memory consumption, and simulation time.

## II. THEORY

As shown in Ref. [2], the Schrödinger equation describing the electronic band structure in one-dimensional (1D) nanostructures in the  $(x-z)$  plane, surrounded by a large vacuum padding in the  $(x-y)$  plane to decouple the structures, using the empirical pseudopotential method is

$$\sum_{\mathbf{G}'} \left( \frac{\hbar^2}{2m} |\mathbf{k} + \mathbf{G}|^2 \delta_{\mathbf{G}'\mathbf{G}} + V_{\mathbf{G}'\mathbf{G}}^{lat} \right) u_{\mathbf{G}'}^{k_z} = E_{k_z} u_{\mathbf{G}}^{k_z}, \quad (1)$$

where  $\mathbf{k} = (0, 0, k_z)$  is the wavevector along the axial  $z$ -direction. This constitutes an eigenvalue problem of rank given by the number of reciprocal-space vectors  $N_{\mathbf{G}}$  within the energy-cutoff sphere of radius  $E_{cut}$ . The QTE describing the 1D electron transport along the  $z$  direction is a linear system of the form

$$(\mathbf{H} - E\mathbf{I} + \Sigma_L + \Sigma_R)\phi = [\mathbf{RHS}]_L^{inj} + [\mathbf{RHS}]_R^{inj}, \quad (2)$$

where  $\mathbf{H}$  is the Hamiltonian for the closed system,  $E$  is the injection energy of electrons,  $\mathbf{I}$  is the identity matrix,  $\Sigma_L$  and  $\Sigma_R$  are the self-energies of the contacts,  $\phi$  is the envelope wavefunction, and  $[\mathbf{RHS}]_L^{inj}$  and  $[\mathbf{RHS}]_R^{inj}$  are the terms representing the amplitudes of the waves injected from

the contacts (self-energies). Using finite difference (FD) and discretizing a device into  $N_z$  slices along the transport direction with a step-size  $\Delta$ , the Hamiltonian  $\mathbf{H}$  takes a block tridiagonal form

$$\mathbf{H} = \begin{bmatrix} \cdot & \cdot & \cdot & \cdot & \cdot & \cdot & \cdot \\ \cdot & \mathbf{T}^- & \mathbf{D}^{i-1} & \mathbf{T}^+ & 0 & 0 & \cdot \\ \cdot & 0 & \mathbf{T}^- & \mathbf{D}^i & \mathbf{T}^+ & 0 & \cdot \\ \cdot & 0 & 0 & \mathbf{T}^- & \mathbf{D}^{i+1} & \mathbf{T}^+ & \cdot \\ \cdot & \cdot & \cdot & \cdot & \cdot & \cdot & \cdot \end{bmatrix}, \quad (3)$$

where the operator  $\mathbf{D}^i$  is a dense matrix of rank  $N_{\mathbf{G}}$  that includes the lattice and external potential (gate and source/drain bias) in the  $i$ -th slice, and the Hermitian operators  $\mathbf{T}^+$  and  $\mathbf{T}^-$  are diagonal matrices also of rank  $N_{\mathbf{G}}$ . Therefore, the rank of  $\mathbf{H}$  is  $N_{\mathbf{G}} \times N_z$ . The self-energy matrix  $\Sigma_L$  is added to  $\mathbf{D}^1$  and  $\Sigma_R$  is added to  $\mathbf{D}^{N_z}$ . Solving Eq. (2) and Poisson's equation self-consistently for different drain-source bias and gate bias, the current-voltage characteristics of the device can be obtained. Since we have not yet implemented in our computer program the capability to account for bound and quasi-bound states, we are unable to perform full self-consistent calculations. Therefore, for now we solve Eq. (2) with an external potential obtained from a self-consistent calculation within a simple semiclassical drift-diffusion approximation. This is performed by solving the two-dimensional Schrödinger equation in all slices, calculating the charge density using local quasi-Fermi level, and then solving Poisson's equation to update the potential. An approximate device current is calculated from the obtained envelope wavefunctions  $\phi$ .

## III. SIMULATIONS AND RESULTS

An atomistic model of an aGNR with six dimer lines along the width direction  $x$  is shown in Fig. 1a and a device model of 6-aGNRFET is shown in Fig. 1b. The channel has  $p^+$  doping and the source and drain contact have  $n^+$  doping. The discretization is shown in Fig. 1c and 1d. The band structure of the 6-aGNR is calculated by solving Eq. (1) and shown in Fig. 2. The self-consistent external potential and charge distribution within the aforementioned semiclassical drift-diffusion simplification are shown in Fig. 3 and their distribution after non-equilibrium quantum transport simulation are shown in Fig. 4. The  $I$ - $V$  characteristics are shown in Fig. 5. Some information about the numerical details of the calculations is shown in Table. I.

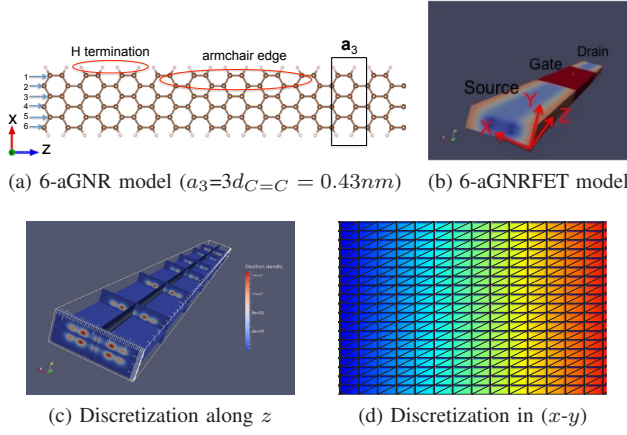


Fig. 1: Device model of 6-aGNRFET with an overall length  $L=30a_3=12.78$  nm, a physical channel length  $L_g=5.12$  nm, a body width  $W=0.62$  nm, and an EOT=0.62 nm. Electron transport is along the  $z$  direction. The device is discretized along  $z$  into  $N_z=121$  slices with  $\Delta=a_3/4=0.11$  nm and discretized in the cross-sectional ( $x$ - $y$ ) plane using a finite element mesh. Notice that this particular triangular mesh is for FFT calculations.

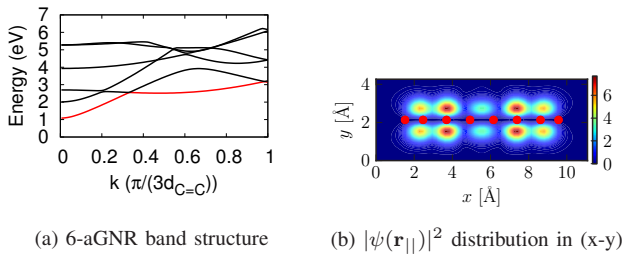


Fig. 2: The electronic dispersion of the first six low-energy conduction bands (CBs) is shown in (a). Within 100 meV from the bottom of the CB, only one conducting channel is observed. The electron probability distribution  $|\psi(\mathbf{r}_{||})|^2$  is shown in (b). This is obtained by averaging the square of the cross-sectional wavefunction over one unit cell along  $z$ . A selected eigenvalue solver from IBM ESSL package is used to calculate the bands in the interesting energy range, and FFT is used to calculate  $|\psi(\mathbf{r}_{||})|^2$  from Eq. (1).

## REFERENCES

- [1] J. Fang, W. Vandenberghe, and M. Fischetti, "Full-band ballistic quantum transport in nanostructures using empirical pseudopotential," in *Computational Electronics (IWCE), 2014 International Workshop on*. IEEE, 2014, pp. 1–3.
- [2] B. Fu and M. Fischetti, "Open boundary-condition ballistic quantum transport using empirical pseudopotentials," in *Computational Electronics (IWCE), 2013 International Workshop on*. IEEE, 2013, pp. 28–29.
- [3] B. Fu, "Quantum transport: from effective mass approximation to full band," Ph.D. dissertation, The University of Texas at Dallas, Richardson, TX, 2013.
- [4] International Technology Roadmap for Semiconductor, "Process integration, devices, and structures," [Online], 2013.

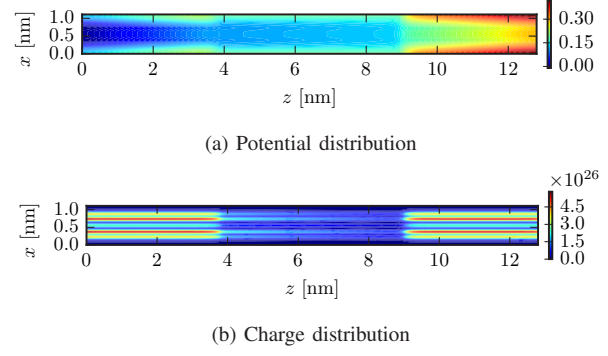


Fig. 3: Approximate potential and charge distribution, averaged along  $y$ , in the ( $x$ - $z$ ) plane after self-consistent calculation with the semiclassical assumption for a 6-aGNRFET with a drain-source bias  $V_{DS}=0.4$  V and a gate bias  $V_{GS}=0.2$  V.

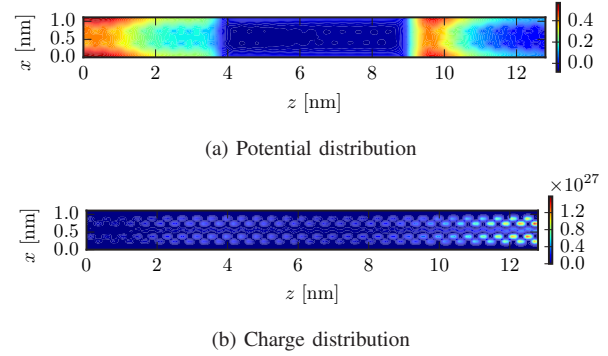


Fig. 4: Potential and charge distribution, averaged along  $y$ , in the ( $x$ - $z$ ) plane from Eq. (2) for a 6-aGNRFET. Quasi-bound states can be observed in the region close to the drain contact. Note that variation of the electron density corresponds to the location of individual atoms.

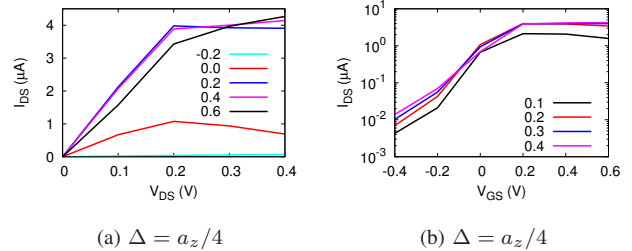


Fig. 5: Current-voltage characteristics of a 6-aGNRFET.

TABLE I: Rank of the matrices, simulation time, and memory consumption when simulating a 6-aGNRFET

| $N_G$ | t (s, Eq. (1)) | t (h)            | LDM   | t (h)            | Memory (GB)      |
|-------|----------------|------------------|-------|------------------|------------------|
| 701   | 10             | 2.5 <sup>a</sup> | 84821 | 0.2 <sup>b</sup> | 5.0 <sup>c</sup> |

<sup>a</sup> Simulation time required to obtain the starting potential self-consistently for each applied bias.

<sup>b</sup> Simulation time required to solve Eq. (2) for a single injection energy  $E$ . MPI is used to solve Eq. (2) in parallel for all the injection energies.

<sup>c</sup> Peak memory required to solve Eq. (2). A sparse matrix solver UMFPACK is used to save memory.